# Development of an ultrasonic pulse-echo (UPE) technique for aircraft icing studies

Cite as: AIP Conference Proceedings **1581**, 1757 (2014); https://doi.org/10.1063/1.4865036
Published Online: 17 February 2015

Yang Liu, Wen-Li Chen, Leonard J. Bond, and Hui Hu

# Development of an Ultrasonic Pulse-Echo (UPE) Technique for Aircraft Icing Studies

Yang Liu[1], Wen-Li Chen[1, 2, 3], Leonard J. Bond[1, 4] and Hui Hu[1]

[1]*Department of Aerospace Engineering, Iowa State University,*
*2271 Howe Hall, Room 1200, Ames, IA 50011, USA*
[2]*School of Civil Engineering, Harbin Institute of Technology,*
*Harbin, Heilongjiang 150090, China*
[3]*Key Lab of Structural Dynamic Behavior and Control (Harbin Institute of Technology), Ministry of Education,*
*Harbin, Heilongjiang 150090, China*
[4]*Center for Nondestructive Evaluation, Iowa State University,*
*1915 Scholl Road, 151 ASC II, Ames, IA 50011, USA*

**Abstract:** Aircraft operating in some cold weather conditions face the risk of icing. Icing poses a threat to flight safety and its management is expensive. Removing light frost on a clear day from a medium-size business jet can cost $300, heavy wet snow removal can cost $3,000 and removal of accumulated frozen/freezing rain can cost close to $10,000. Understanding conditions that lead to severe icing events is important and challenging. When an aircraft or rotorcraft flies in a cold climate, some of the super cooled droplets impinging on exposed aircraft surfaces may flow along the surface prior to freezing and give various forms and shapes of ice. The runback behavior of a water film on an aircraft affects the morphology of ice accretion and the rate of formation. In this study, we report the recent progress to develop an Ultrasonic Pulse-Echo (UPE) technique to provide real-time thickness distribution measurements of surface water flows driven by boundary layer airflows for aircraft icing studies. A series of initial experimental investigations are conducted in an ice wind tunnel employing an array of ultrasonic transducers placed underneath the surface of a flat plate. The water runback behavior on the plate is evaluated by measuring the thickness profile variation of the water film along the surface by using the UPE technique under various wind speed and flow rate conditions.

**Keywords:** Aircraft Icing, Ultrasonic Pulse-Echo, Water Film Thickness
**PACS:** *43.35.Zc, 81.70.Cv, 47.85.Gj, 89.40.Dd, 89.40.Cc

## INTRODUCTION

Aircraft operating at high altitude in cold weathers can encounter super-cooled clouds or precipitation droplets, which cause ideal icing conditions. Therefore, aircraft in such situations are facing possible icing events that can severely affect the flight performance of the aircraft. Generally, icing can significantly increase drag, decrease lift, and cause control problems [1]. To minimize the effect of icing, an ice management approach is necessary. For operations, the cost for ice removal/deicing can impact flight economics. An investigation by the National Business Aviation Association (NBAA), found that cleaning light ice or snow from a light aircraft like a Cessna 172 typically costs $160, removing light frost from a medium-sized business jet on a clear day costs $300, removal of heavy wet snow costs $3,000, and removal of frozen/freezing rain can cost close to $10,000.

The ice morphology depends on the weather conditions; the icing process may be either rime ice or glaze ice growth [2]. Rime ice forms with lower super-cooled liquid water content (LWC) and smaller droplets at lower temperatures, when the heat transfer from the ice surface is adequate to remove all of the latent heat of the impinging droplets; whereas glaze ice is generally created with high LWC and large droplet size at higher temperatures, when the heat transfer is inadequate to remove all of the latent heat from the impinging droplets [3]. In rime ice accretion, the impinging super-cooled water droplets rapidly freeze on impact with the surface causing ice conforming to the exterior shape with a much greater roughness than that of the component surface. However in glaze ice growth, the impinging droplets won't freeze immediately on impact and water may run back over the component surface or existing ice surface before freezing further downstream, which as a result can cause a shape with pronounced horns and with a translucent appearance that projects into the incoming flow [2]. Thus the most significant aircraft flight performance deficit is related to glaze ice formation.

As shown in Figure 1, in the process of glaze ice formation on an aircraft surface, water and air boundary layers are simultaneously disturbed by the accretion and deformation of the ice layer. In the meantime, the interaction

*40th Annual Review of Progress in Quantitative Nondestructive Evaluation*
AIP Conf. Proc. 1581, 1757-1764 (2014); doi: 10.1063/1.4865036

between air and water flows significantly affects the ice formation and accretion process. Monitoring of the water film flow behavior is therefore of great importance in the investigation of glaze ice formation. This behavior can be investigated by measuring the thickness profile variation of the water film in real time. In the past several decades, various experimental techniques have been developed to measure the thickness distribution of the liquid water free surface, with optical measurement techniques being the most commonly applied. These have the advantage of being non-intrusive while performing instantaneous measurements over a monitored area [4]. However, most of the optical techniques require the addition of marker particles into the liquid flow so as to provide points for optical measurement. This requirement, to some extent, may affect the fluid properties and flow characteristics. Moreover, it is not feasible to add such marker particles when measuring the water film thickness on a flying aircraft wing. Besides the marker particle issue, optical measurement techniques are limited by the capabilities of the cameras used. Although a surface thickness distribution can be easily reconstructed, single point data are more difficult to obtain.

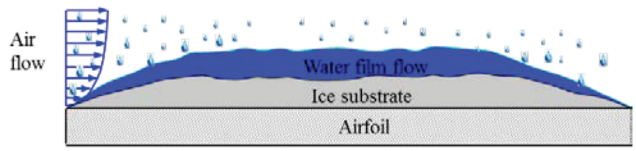


**FIGURE 1.** A schematic of glaze ice formation and accretion.

Over the years, ultrasonic techniques have been widely applied in measuring thickness of solid objects, including solidification processes and a range of membrane processes, including the growth of fouling layers [5, 6]. Other examples of ultrasonic applications include work by Kamei and Serizawa [7], which measured the liquid film flow around a nuclear fuel rod. Li and Serizawa reported an experimental study on flow characteristics of a vertically falling film flow of a liquid metal in a transverse magnetic field [8]. In 2010, an ultrasonic transmission thickness measurement system (UTTMS) was developed to characterize the water rivulets on stay cables suffering from wind-rain-induced vibration [9], and there has been previous work to monitor ice growth and thickness [10-14]. Such ultrasonic techniques can not only provide excellent time resolution in single-point measurement, but also provide good spatial resolution over an area by using an array of transducers.

This paper is organized in four sections. Section 2 describes the measurement principle for Ultrasonic Pulse-Echo (UPE), which has also been called acoustic time domain reflectometry (ATDR), and the experimental setup for wind-driven water film flow thickness measurement. Section 3 presents the measurement results and discussions, including single-point thickness variation and the corresponding Fast Fourier Transform (FFT) analysis of surface displacement, instantaneous water film profile variation in the center line, and time-averaged thickness distribution over the monitored area. Finally, section 4 presents some conclusions.

## MEASUREMENT PRINCIPLE AND EXPERIMENTAL SETUP

### Ultrasonic Pulse-Echo (UPE) System

An Ultrasonic Pulse-Echo (UPE) technique is used to investigate the runback behavior of water film and ice accretion characteristics, under the influence of air flow. The UPE system provides accurate and high efficient data collection, enables monitoring of water film thickness variation at selected locations. By averaging the thickness values at each monitored point, the time-averaged thickness distribution can be reconstructed. The previous investigations measuring liquid thickness using UT techniques have validated the feasibility of the techniques [7-9].

The UPE system is shown schematically in Figure 2. The central element of the UPE system is a multichannel inspection system, an Omniscan iX [15]. It has the capability to send control signals and deliver high voltage pulses to act as a multiplexer to operate with multiple ultrasonic transducers. With the high voltage excitation, the transducers emit ultrasonic waves, which then reflected at the interfaces in the measured object. The reflected waves are then detected using the same transducers and signals monitored by a PC.

Eight fingertip case style transducers (0.125 inch element diameter) with a crystal oscillator frequency of 10 MHz are used. The set pulse repetition frequency (PRF), which is the multiplexer step frequency, is 750Hz.


**FIGURE 2.** Schematic of UPE system.

## Measurement Principle and Calibration

Ultrasonic waves emitted by the transducers are reflected at the interfaces of two different materials, such as the airfoil-ice interface, ice-water interface and water-air interface in the aircraft icing detection application. In this study, the wind-driven water film flows on a flat plate with transducers placing underneath the plate as shown in Figure 3. The various pulse and echoes are illustrated in Fig. 3. The principle of the water film thickness measurement using UPE is based on the time-of-flight: $\delta = V \times t / 2$, where $\delta$ is the thickness of the measuring water film, $V$ is the propagation velocity of the ultrasonic wave in water, and $t$ is the time elapsed between the first echo and the second echo return from the two interfaces (wall-water interface and water-air interface). The measurement accuracy is limited by the digitizing frequency of the multiple channel inspection system and assumed wave velocity in water used, which is a function of temperature. In this experiment, the digitizing frequency is 100MHz. Combined with the speed of sound in water at 20℃ of 1483m/s [5], the estimated accuracy of the measurement is of the order of ±5μm.

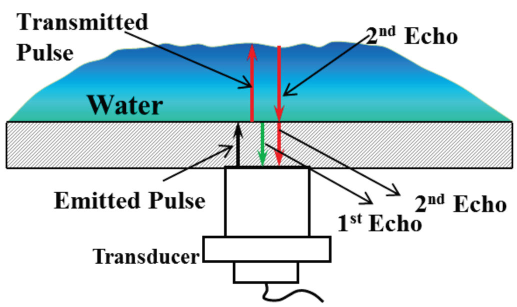


**FIGURE 3.** A schematic of Ultrasonic Pulse-Echo technique.

In order to validate the reliability of the water thickness measurement using UPE in this paper, a set of different depths of water in a tank were measured using the UPE system and compared with data from a depth gauge. The water depths were measured five times by the two methods for every depth, and the mean depth values were compared as shown in Figure 4. The maximum standard error of the mean depths using UPE is smaller than 0.005mm, while that by the depth gauge is smaller than 0.12mm. The results data measured by the two methods are in very good agreement, indicating that the UPE system is a reliable and accurate tool for measuring water thickness.

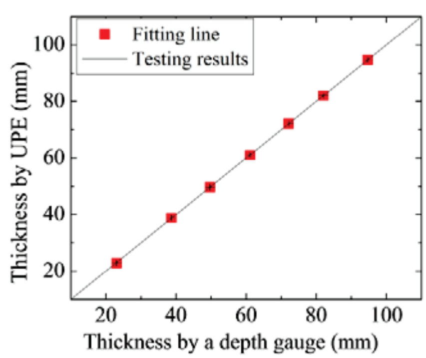


**FIGURE 4.** Comparison of water depth measured by UPE and a depth gauge.

## Experiment Setup and Procedure

The schematic of experiment setup used in the thickness measurement of wind-driven water film is shown as Figure 5. The plate is placed in the test section of an ice wind tunnel; ultrasonic transducers are located underneath the test plate as shown in Fig. 5. A water supply system including reservoir, digital gear pump, water tank, and water collector is arranged as illustrated in the figure. The water tank is used to provide steady water flow under different water flow rates controlled by the digital gear pump (Cole-Parmer 75211-30). While measuring the thickness variation of the wind-driven water film flow by the UPE system, a high-speed camera is also used for flow visualization so as to provide simultaneous flow information. In order to generate a uniform water film flow, a line of water outlet holes is designed on the test plate as shown in Figure 6. The width of the water outlet area is W=76.2mm, with the hole diameter of d=2.032mm and spacing distance of b=6.35mm. In addition there are 150 flat bottom holes of 3.05mm depth which can serve as transducer locations in the bottom of the plate.

The measurement was performed with the water flow rates of 250, 300 and 350ml/min, and when setting the wind speed at 5, 10, 15 and 20m/s at each flow rate to investigate the water film behavior under different conditions. For each experiment, eight transducers were employed to monitor water film thickness variation at eight points set in a line along the flow direction. The data recording time for each case is 30s to ensure that adequate measurement of the thickness variation is monitored.

In each experiment, the eight transducers are placed in a certain line first, and then the water flow rate is adjusted to 250ml/min. Measurements are then performed under different wind speeds (5, 10, 15 and 20m/s). The water flow rates will then be adjusted to 300 and 350ml/min and the measurement process repeated. When this sequence of measurements is completed, the eight transducers are switched to another line and the process repeated. For the preliminary measurements, five lines of transducer locations were studied.

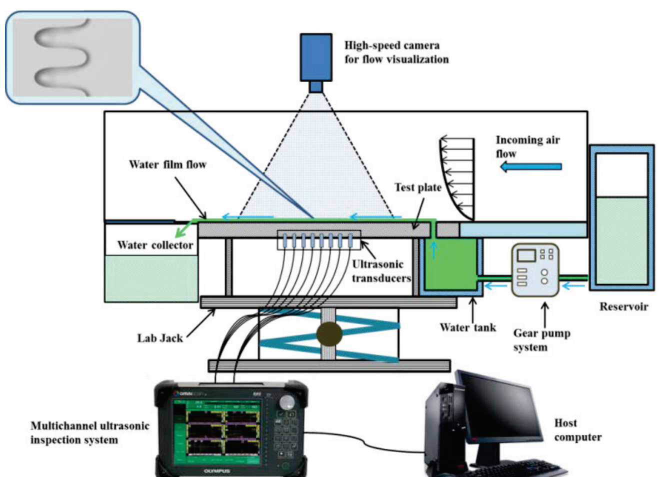


**FIGURE 5.** Schematic of experiment setup for wind-driven water film flow monitoring by UPE.

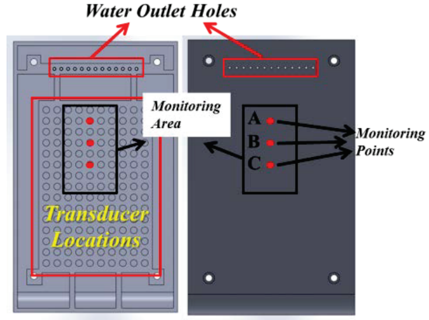


**FIGURE 6.** Design of test plate with transducer locations and water outlet holes.

## EXPERIMENTAL RESULTS AND DISCUSSIONS

The monitoring area and three monitoring points A, B, and C are shown in Figure 6. The monitoring points are located at different positions along the centerline. In this study, a three-level analysis of data is performed as follows: 1, Single-point thickness variation and corresponding Fast Fourier Transform (FFT) analysis; 2, instantaneous water film profile variation in the center line; and 3, time-averaged thickness distribution over the monitoring area. In these analyses, the coordinate positions are all nondimensionalized and given as a function of the width of the monitored area.

### Single-Point Thickness Variation Analysis

The water film thickness variation history and corresponding spectrum at three monitoring points under the experiment condition of Q=250ml/min & V=5m/s are shown in Figure 7. At a wind speed of 5m/s, the water film flow is relatively stable; however a small surface wave motion can be observed at the water-air interface. As a result, a dominant frequency of 15.06±0.02Hz at different monitoring points can be extracted from the calculated spectrum, although the measured thickness seems nearly constant at 1mm, when the thickness variation history is examined. The near identical dominant frequency measured at different points indicates that the water film flows with just small interfacial fluctuation, and it is consistent along the flow direction.

With the wind speed increasing to 10m/s at the same flow rate, a distinct fluctuation of the water-air interface appears throughout the monitoring area. In addition, a periodical wave mode can be seen. This is verified by the frequency spectrum as shown in Figure 8. The same frequency [15.06±0.02Hz] as that at the wind speed of 5m/s dominates in the water film flow, indicating the periodicity of the water-air interfacial wave remains uniform at low wind speed under 10m/s. Based on the dominant frequency obtained, a period of the interfacial wave of T=0.0664±0.0013s can be estimated.

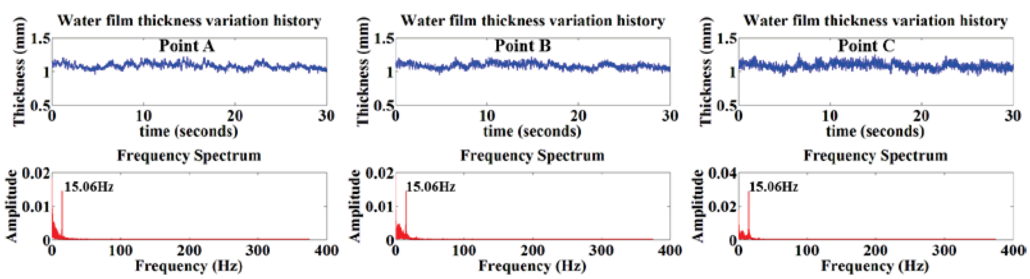


**FIGURE 7.** Thickness variation history and FFT analysis at Q=250ml/min & V=5m/s.

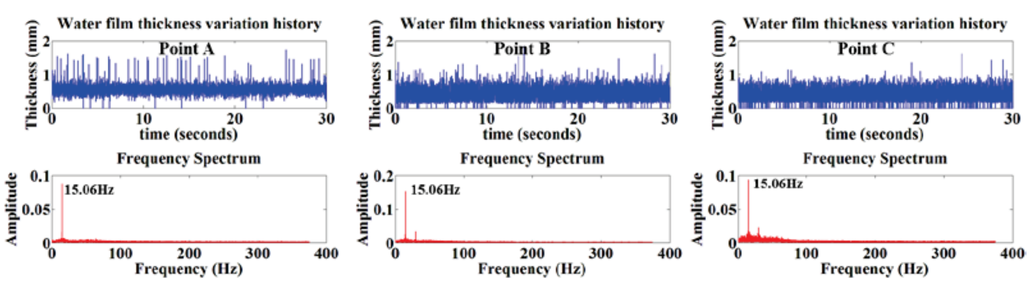


**FIGURE 8.** Thickness variation history and FFT analysis at Q=250ml/min & V=10m/s.

The water film thickness variation history and corresponding spectrum at the wind speed of 15 and 20m/s are shown in Figure 9 and Figure 10 respectively. At a higher wind speed, the interfacial fluctuation becomes dramatically volatile and only weak or even no periodical water wave in the film flow can be found in the monitored area. A possible reason is that the water film flow becomes turbulent for wind speeds above 15m/s, which is more essential to dissipate the energy and makes the water film flow unpredictable.

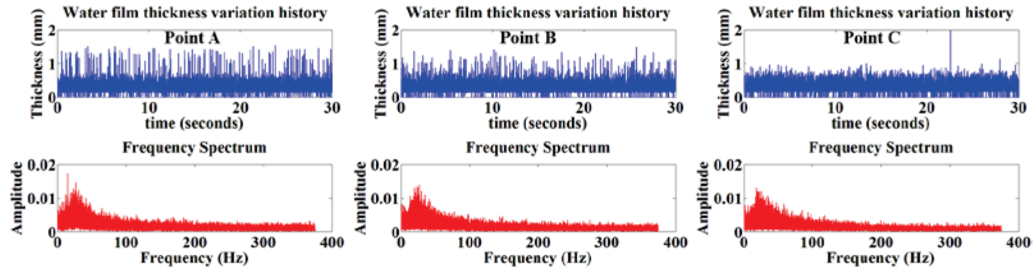


**FIGURE 9.** Thickness variation history and FFT analysis at Q=250ml/min & V=15m/s.

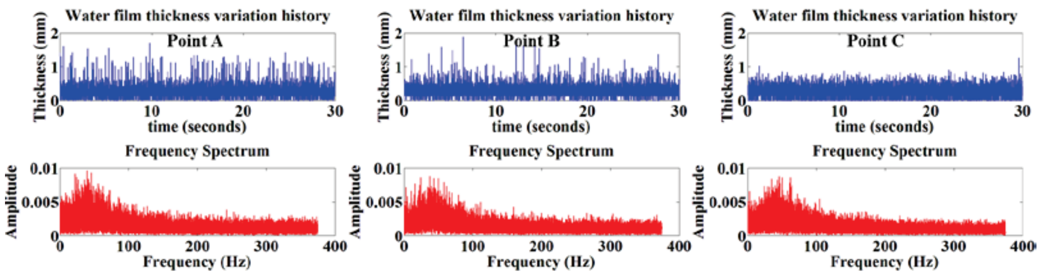


**FIGURE 10.** Thickness variation history and FFT analysis at Q=250ml/min & V=20m/s.

## Instantaneous Water Film Profile Variation in Center Line

Based on the discussion in the single-point thickness variation analysis, a wave period of T=0.0664±0.0013s can be estimated at the wind speed of 10m/s. Therefore, a complete period of the interfacial wave is extracted from the collected experiment data. Five typical phases are selected in one period with data recording time points from $t_0$=0.6973s to $t_f$=0.7627s. The thickness variation profiles at other wind speeds are correspondingly illustrated at the same time points, as presented in Figure 11.

At the wind speed of 5m/s, the thickness profiles at different times are almost the same, indicating that the water film flow at this wind speed is relatively stable; however a slight periodical fluctuation exists at the water-air interface. This result is consistent with that in the single-point thickness variation analysis. When the wind speed goes up to 10m/s, a comprehensive phase development comes into sight. A phase shift with time can be observed, which has good agreement with the result in previous analysis. At a wind speed above 15m/s, the periodical characterization is not clear, and the interfacial fluctuation is extremely complicated. This needs to be further investigated.

In addition, the equilibrium position of interfacial waves tends to decrease with wind speed increasing as shown in the figure. This is related to the mass conservation, which is discussed in the following section.

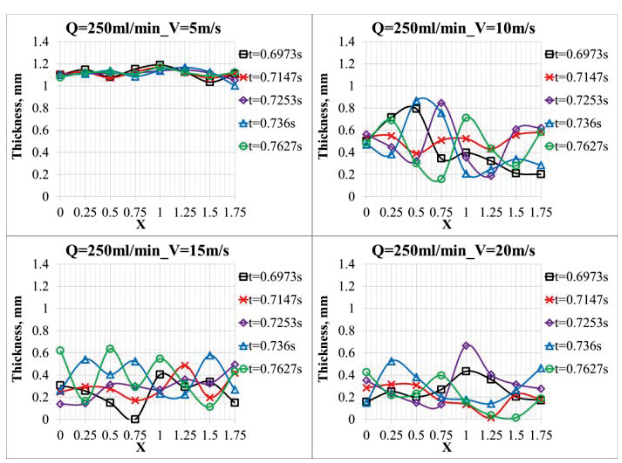


**FIGURE 11.** Water film profile variation in an approximate period.

## Time-Averaged Thickness Distribution

In order to evaluate the thickness distribution characterization of the wind-driven water film flow, a series of time-averaged thickness reconstructions using average thickness values recorded during 30s periods at every single measuring point within the monitoring area were used.

The film thickness distribution at the flow rate of 250ml/min at different wind speeds are shown in Figure 12. It is obvious that with the wind speed increasing, the averaged thickness distribution becomes thinner. When the supplied flow rate of the water film flow is fixed, a higher wind speed indicates a smaller film cross section area according to the mass conservation equation, which consequently results in a thinner thickness distribution. At a wind speed of 5m/s, the average thickness is about 1mm, which then decreases to 0.6, 0.4 and 0.2mm at 10, 15 and 20m/s, respectively.

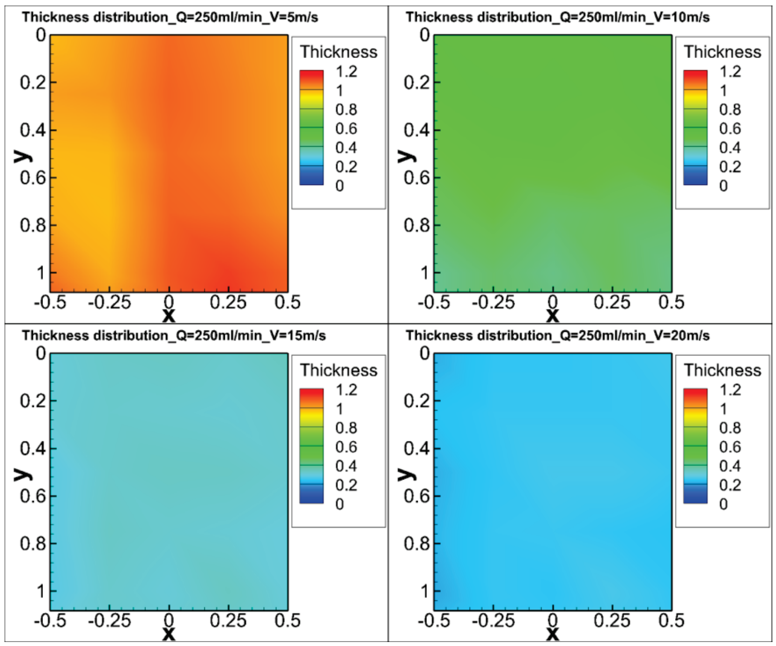


**FIGURE 12.** Water film thickness distribution at Q=250ml/min.

## CONCLUSIONS

An Ultrasonic Pulse-Echo (UPE) technique was developed, calibrated and used to measure thickness of wind-driven water films. The feasibility and implementation of the UPE system was demonstrated by measuring the thickness variation of the water film flow. The results indicate that the UPE system is a reliable technique in measuring water film thickness with high accuracy and excellent time resolution. A three-level analysis was performed and some physical phenomena are revealed in the wind-driven water film flow.

For the thickness variation at a single-point, the water film variation history and corresponding spectrum at three monitoring points along the flow direction in centerline are analyzed. A clear dominant frequency is revealed at the wind speed of 5 and 10m/s, indicating that a periodical water-air interfacial wave exists at a low wind speed below 10m/s. However, no well-defined dominant frequency is found at 15 or 20m/s. At such wind speeds, the interfacial fluctuation is strong and erratic, which may result from turbulent flow, causing a chaotic thickness variation.

For the instantaneous water film profile variation along the center line, according to the thickness profile variation at 5 and 10m/s, a complete period of the interfacial wave is extracted with five typical phases selected within the 30 second measurement period. At the wind speed of 5m/s, the thickness profile fluctuation is slight, ensuring a stable water film flow over the surface. As wind speed goes above 15m/s, no periodical characterization can be isolated, although the interfacial fluctuation is very strong.

For the time-averaged thickness distribution, with the wind speed increasing at each flow rate, the thickness distribution comes to be thinner. Moreover, the time-averaged thickness distribution seems to be more uniform at a higher wind speed compared with that at a low speed.

## ACKNOWLEDGMENTS

The project is mostly funded by National Science Foundation (NSF) under award number CBET-1064196. The authors also want to thank Mr. Kai Zhang of Iowa State University for his help in manufacturing the test models and setting of the experiments. Equipment support is provided through the NSF IU CRC Center for Nondestructive Evaluation, Iowa State University.

## REFERENCES

1. T. Cebeci, F. Kafyeke, Aircraft icing, Annual review of fluid mechanics, 35 (2003) 11-21.
2. R.W. Gent, N.P. Dart, J.T. Cansdale, Aircraft icing, Philosophical Transactions of the Royal Society of London Series a-Mathematical Physical and Engineering Sciences, 358 (2000) 2873-2911.
3. R.J. Hansman, M.S. Kirby, D.-W. Zhang, F.-S. Wei, Comparison of wet and dry growth in artificial and flight icing conditions, Journal of Thermophysics and Heat Transfer, 1 (1987) 215-221.
4. G. Gomit, L. Chatellier, D. Calluaud, L. David, Free surface measurement by stereo-refraction, Experiments in Fluids, 54 (2013) 1-11.
5. D. Ensminger, and L.J. Bond, Ultrasonics: Fundamentals, Technologies, and Applications, 3rd Edition, CRC Press, Taylor and Francis Group (Boca Raton), 2011.
6. A.P. Mairal, A.R. Greenberg, W.B. Krantz, L.J. Bond, Real-time measurement of inorganic fouling of RO desalination membranes using ultrasonic time-domain reflectometry, Journal of membrane Science, 159 (1999) 185-196.
7. T. Kamei, A. Serizawa, Measurement of 2-dimensional local instantaneous liquid film thickness around simulated nuclear fuel rod by ultrasonic transmission technique, Nuclear engineering and design, 184 (1998) 349-362.
8. F.-C. Li, A. Serizawa, Experimental study on flow characteristics of a vertically falling film flow of liquid metal NaK in a transverse magnetic field, Fusion engineering and design, 70 (2004) 185-199.
9. F.-C. Li, W.-L. Chen, H. Li, R. Zhang, An ultrasonic transmission thickness measurement system for study of water rivulets characteristics of stay cables suffering from wind–rain-induced vibration, Sensors and Actuators A: Physical, 159 (2010) 12-23.
10. R.J. Hansman, M.S. Kirby, Measurement of ice accretion using ultrasonic pulse-echo techniques, Journal of Aircraft, 22 (1985) 530-535.
11. R.J. Hansman, M.S. Kirby, Measurement of ice growth during simulated and natural icing conditions using ultrasonic pulse-echo techniques, Journal of Aircraft, 23 (1986) 492-498.
12. R.J. Hansman, M.S. Kirby, R.C. McKnight, R.L. Humes, In-flight measurement of airfoil icing using an array of ultrasonic transducers, Journal of Aircraft, 25 (1988) 531-537.
13. R.J.O.H.N.J.R. Hansman, M. Kirby, F. Lichtenfelts, Ultrasonic techniques for aircraft ice accretion measurement, (1990).
14. Q. Liu, K.T. Wu, M. Kobayashi, C.K. Jen, N. Mrad, In situ ice and structure thickness monitoring using integrated and flexible ultrasonic transducers, Smart Materials & Structures, 17 (2008).
15. Omniscan®iX Conventional Ultrasound User's Manual, DMTA037-01EN-Revision A, Olympus NDT Canada Inc. (2007).